Electronic Supplementary Material (ESI) for Polymer Chemistry.

Supplementary Information

Thermoresponsive Hydrogels Formed by Poly(oxazoline) Triblock Copolymers

Bryn D. Monnery* and Richard Hoogenboom*

Supramolecular Chemistry Group, Centre of Macromolecular Chemistry (CMaC), Department of Organic and Macromolecular Chemistry, Ghent University, Krijgslaan 281 - S4, 9000 Gent, Belgium. bryn.monnery@gmail.com; Richard.Hoogenboom@UGent.be

^{1}H-NMR Characterisation of Triblock Copolymers

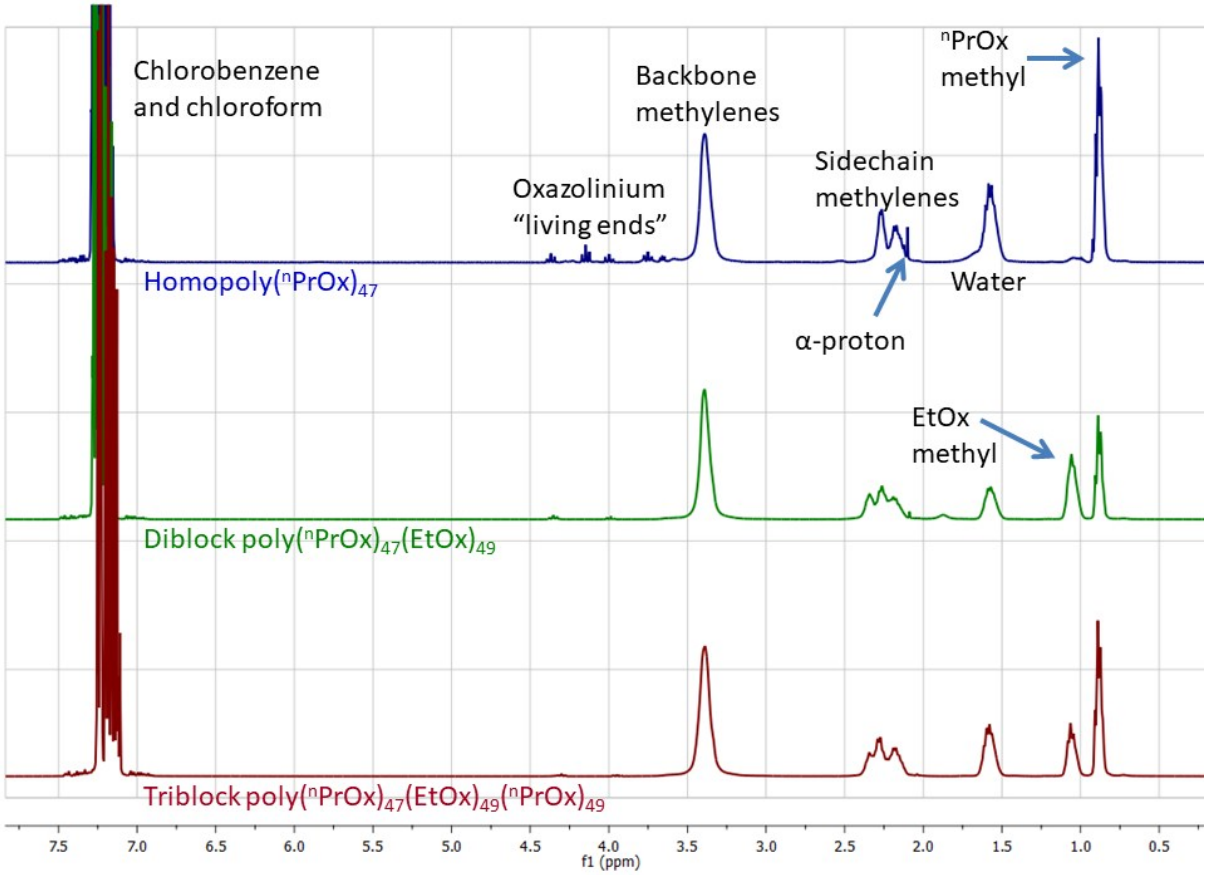

Figure S1: ^{1}H-NMR of the P1 1st block (homopolymer), 1st and 2nd blocks (diblock) and all three blocks (triblock). Percentage molar composition was determined from the monomer content at the various stages, and final composition by conversion to weight percentages and multiplication of final product molar mass.

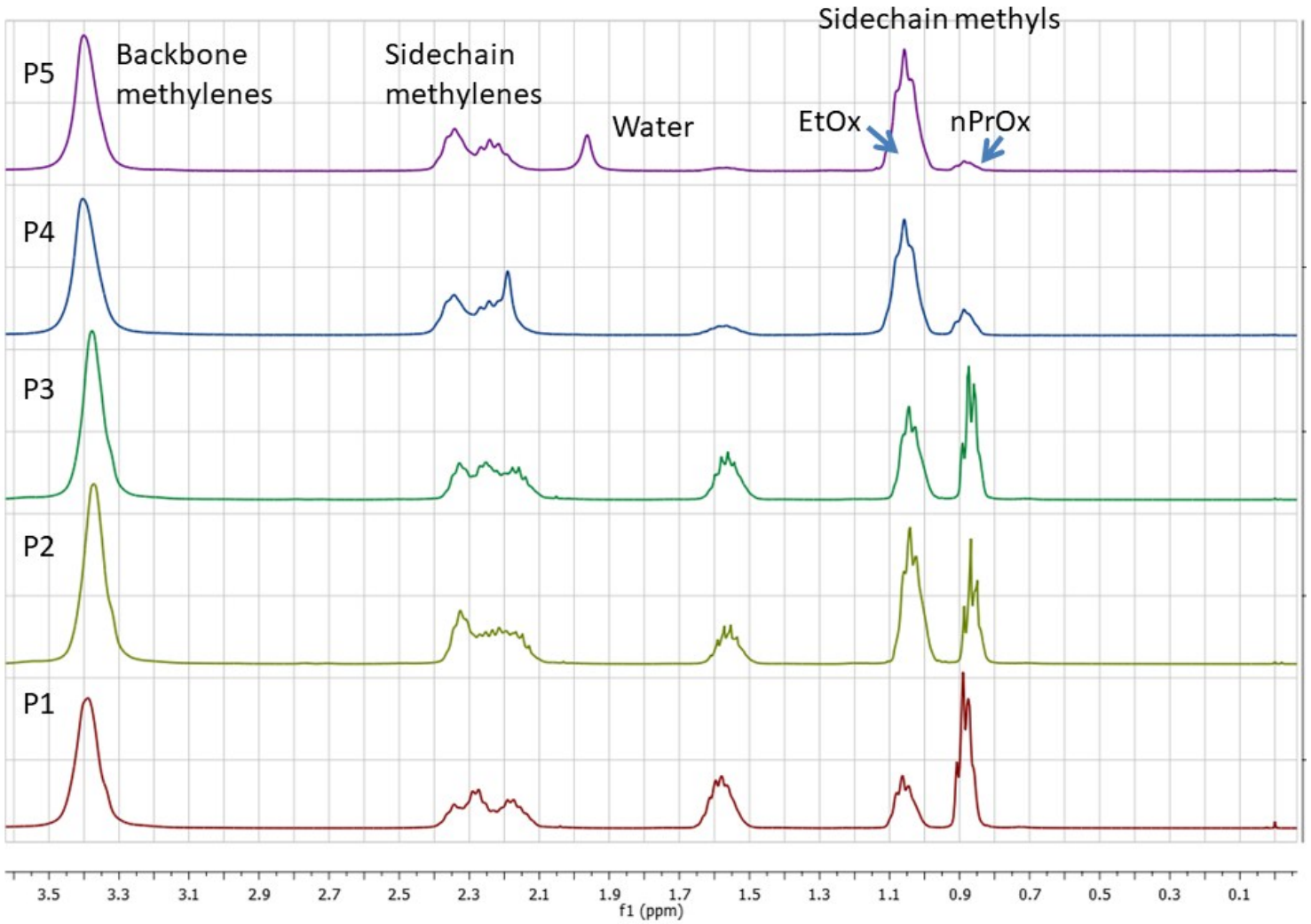

Figure S2: 1H-NMR of final triblocks P1-5, showing decreasing nPrOx content

Feedstocks for P1-5

Table S1: Feedstocks for synthesis of P1-5

	Initiator (HPhOxBF4)		M1 (nPrOx)				M2 (EtOx)				M3 (nPrOx)			
	mg	mmol	ml	mmol	ratio	Rxn Time (hrs)	ml	mmol	ratio	Rxn Time (hrs)	ml	mmol	ratio	Rxn Time (hrs)
P1	234.20	0.93	5.40	46.80	50.34	166	5.00	49.40	53.13	169	5.40	46.80	50.34	287
P2	118.60	0.47	2.70	23.40	49.70	190	5.00	49.40	104.92	336	2.70	23.40	49.70	166
P3	59.30	0.24	1.40	12.10	51.40	169	5.00	49.40	209.85	672	1.40	12.10	51.40	164
P4	24.89	0.10	1.13	9.79	99.08	218	10.50	103.80	1050.51	504	1.13	9.79	99.08	353
P5	13.55	0.05	0.62	5.37	99.83	218	11.40	112.70	2095.14	1008	0.62	5.37	99.83	168

SEC of Homopoly(nPrOx) of DP= 50 and 100

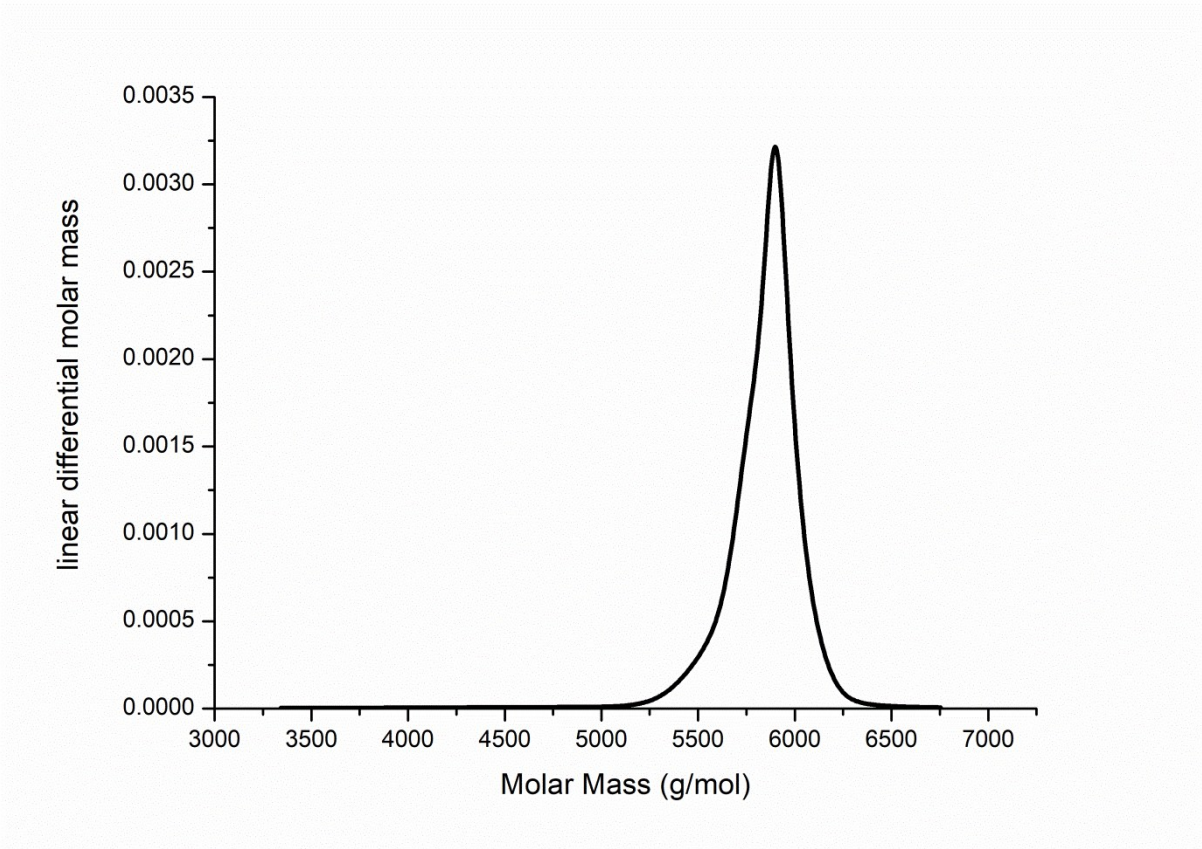

Figure S3: SEC-MALS molar mass distribution of a DP = 50 homopolymer of nPrOx.

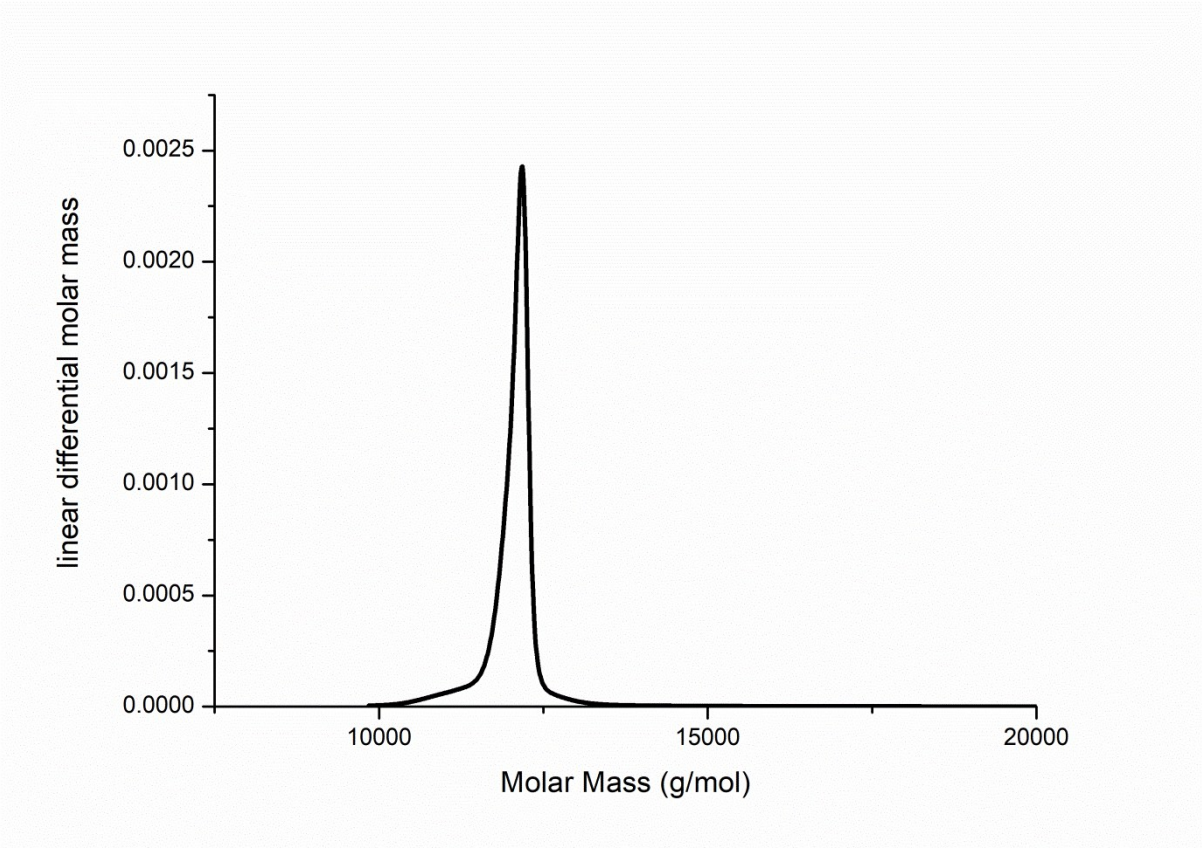

Figure S4: SEC-MALS molar mass distribution of a DP = 100 homopolymer of nPrOx.

Example of results of difunctional initiation

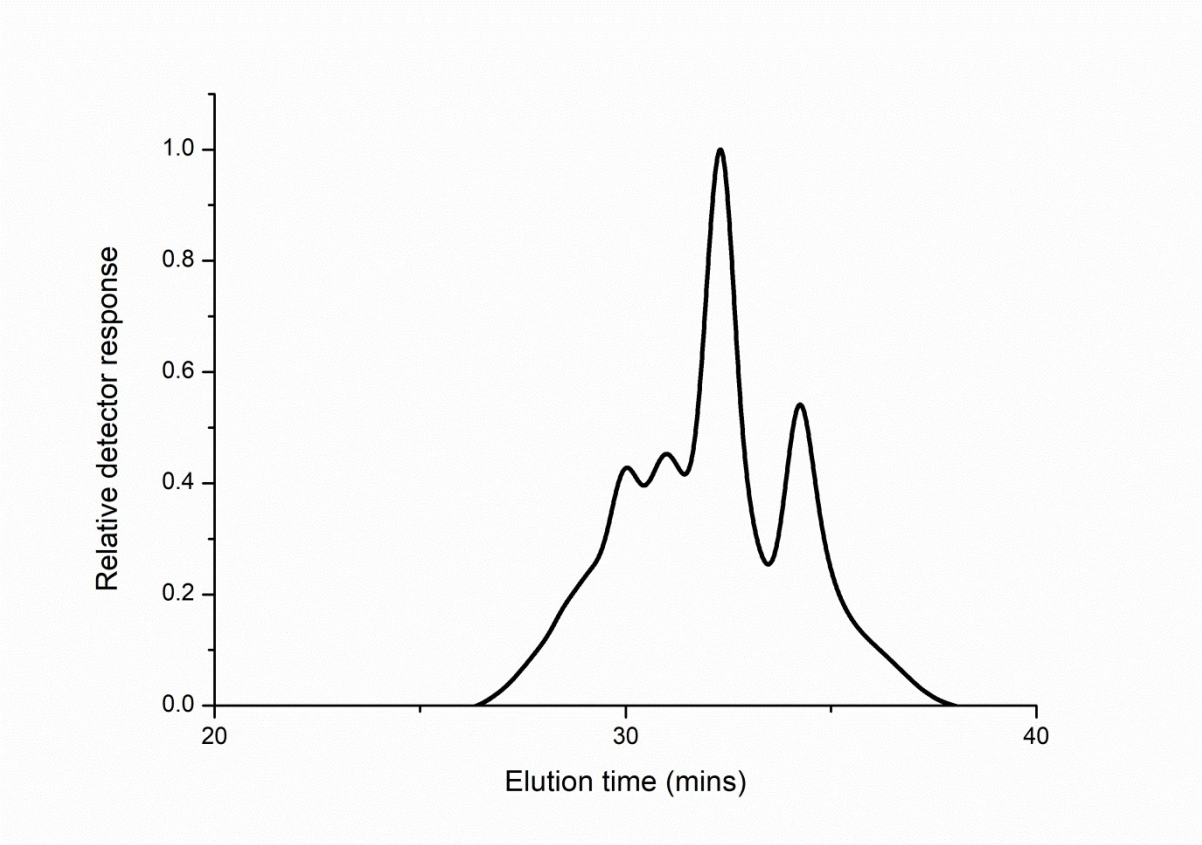

Figure S5: SEC-RI eluogram of an attempted triblock synthesised by a 250:1 ratio of EtOx to butyl ditriflate being allowed to react to completion, followed by a 25:1 ratio of ^{n}PrOx being distilled in and allowed to react to completion. Clearly there is considerable one-ended initiation and the product is extremely impure.

Dynamic Light Scattering

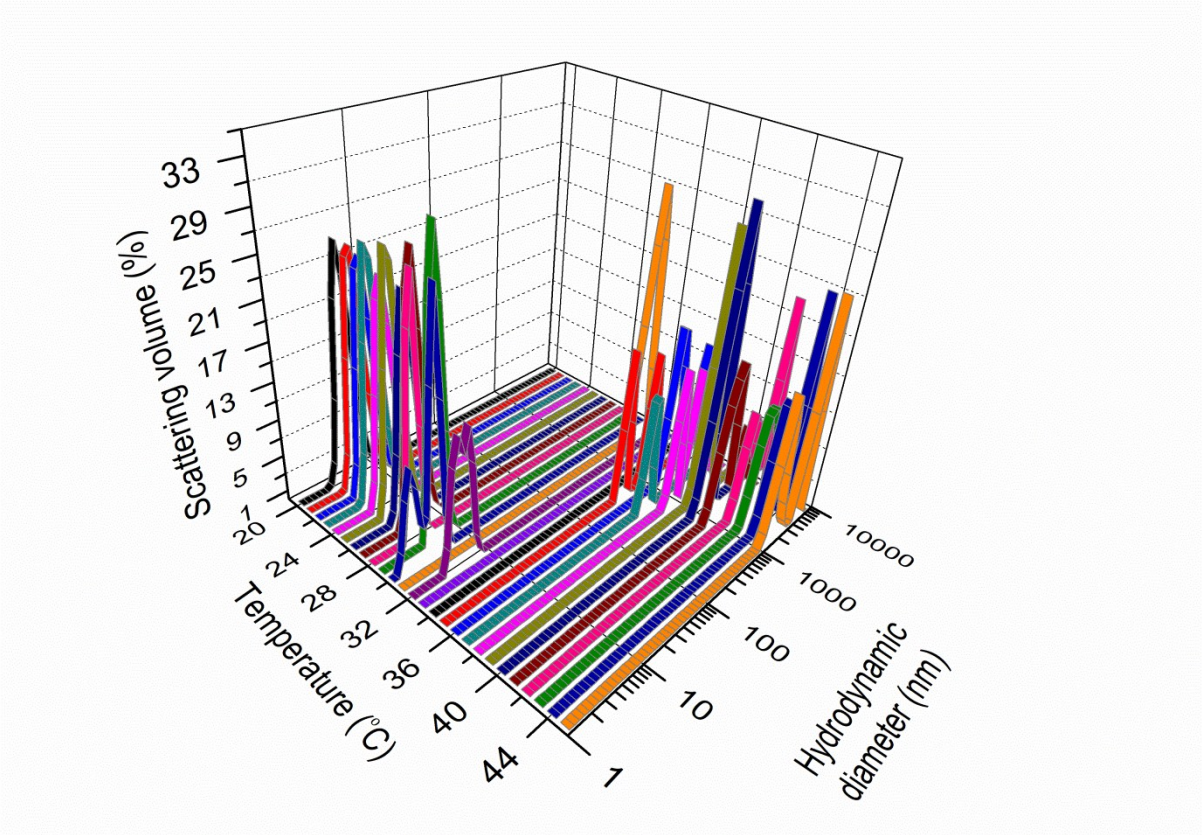

Figure S6: Temperature scanned dynamic light scattering volume plot of P1. The polymer exists as a free chain until ca. 31 ^{o}C, when the polymer aggregates.

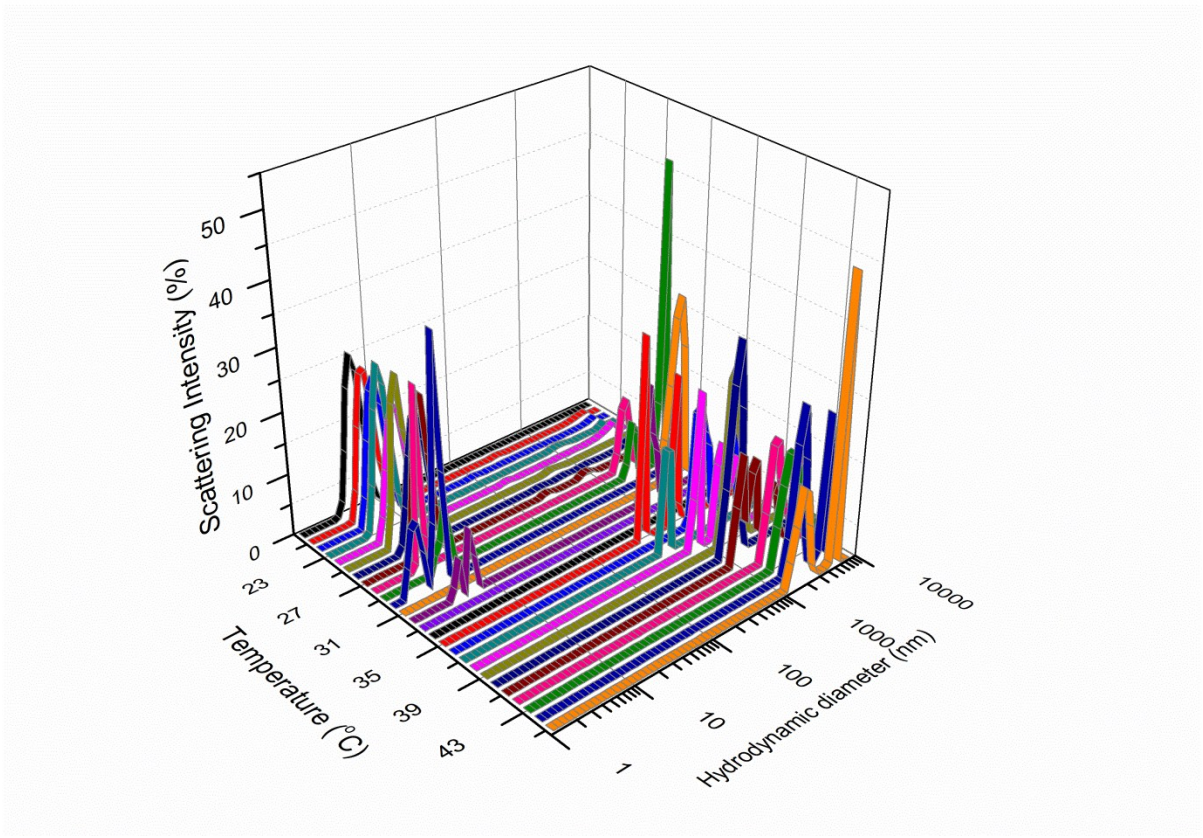

Figure S7: Intensity plot of P1 (*cf.* Fig. S6) which reveals low concentrations of aggregates, even below the T_{CP} of the outer blocks.

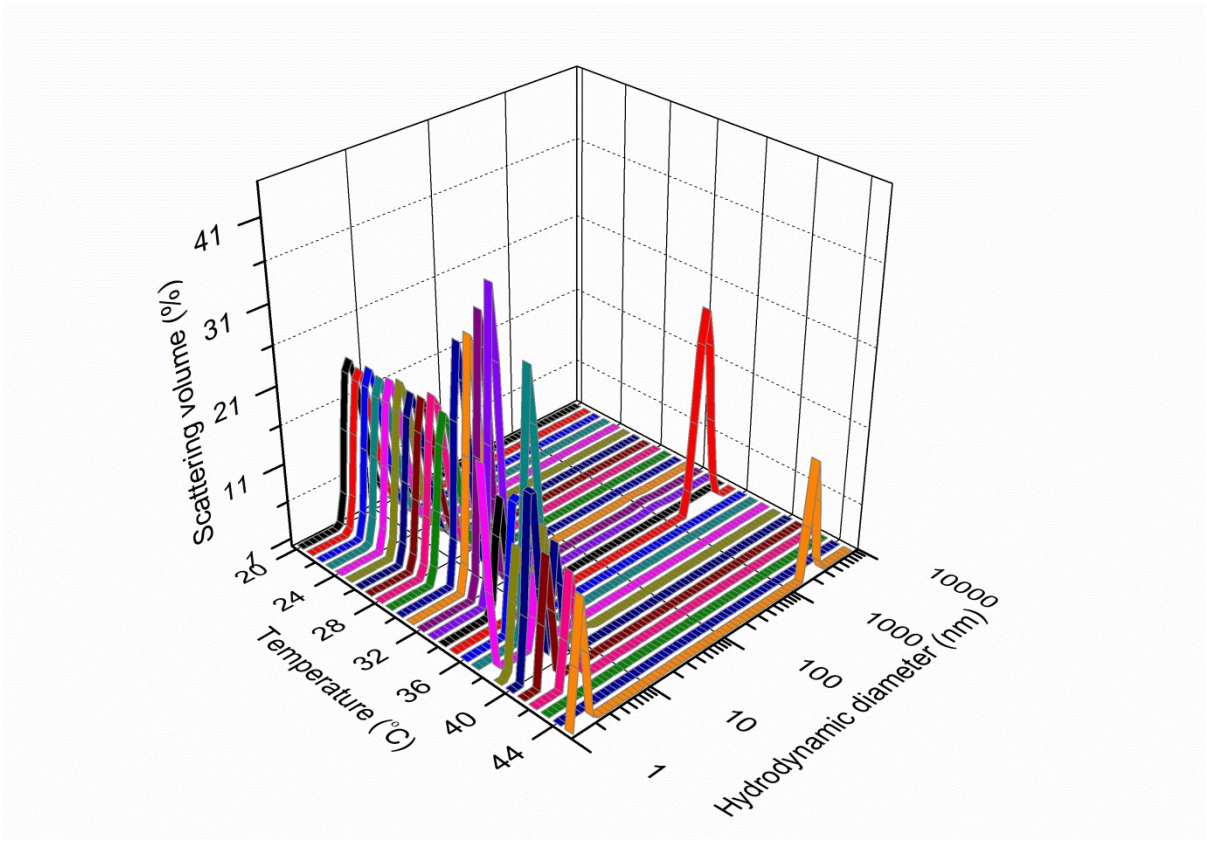

Figure S8: Temperature scanned dynamic light scattering volume plot of P2. The polymer exists as a free chain, and starts to compact at ca. 35 ^{o}C, indicating the polymers outer blocks are self-aggregating.

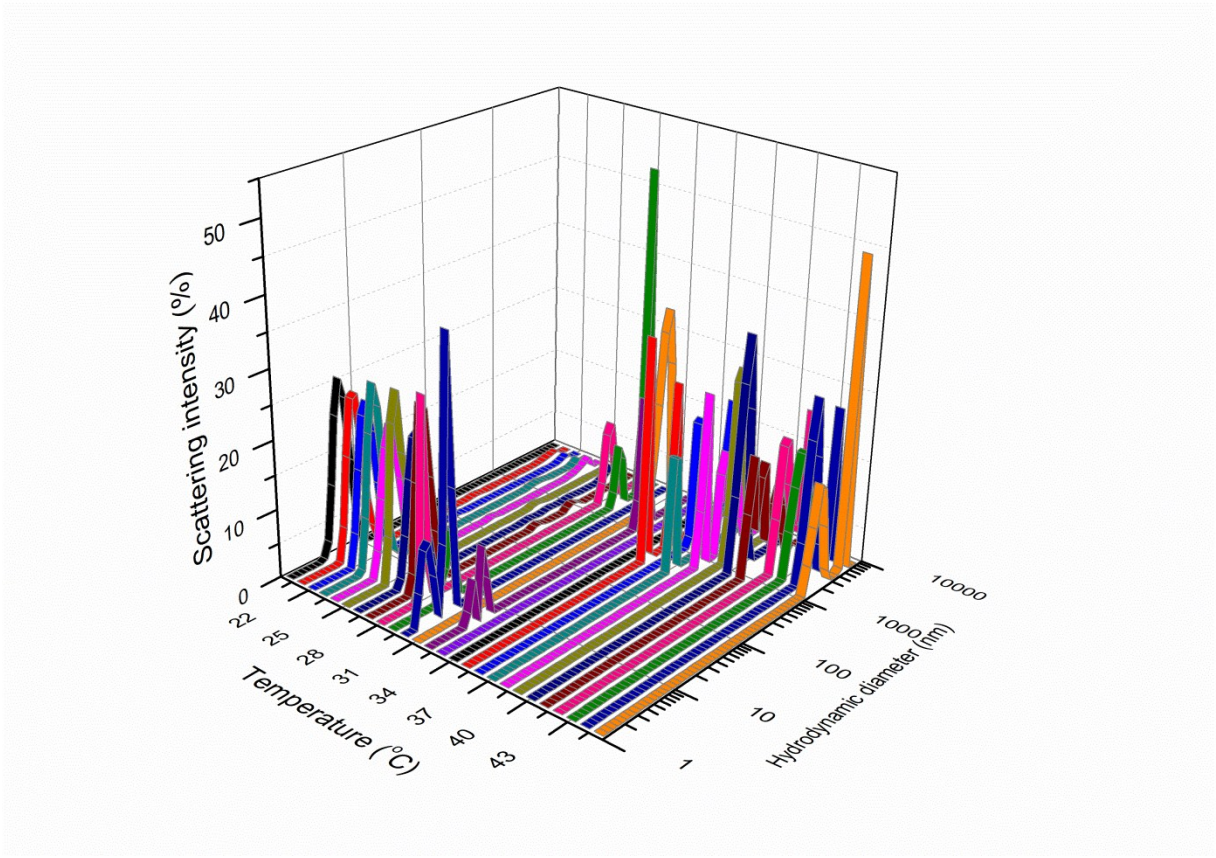

Figure S9: Intensity plot of P2 (*cf.* Fig. S8) which also reveals low concentrations of aggregates, even below the T_{CP} of the outer blocks.

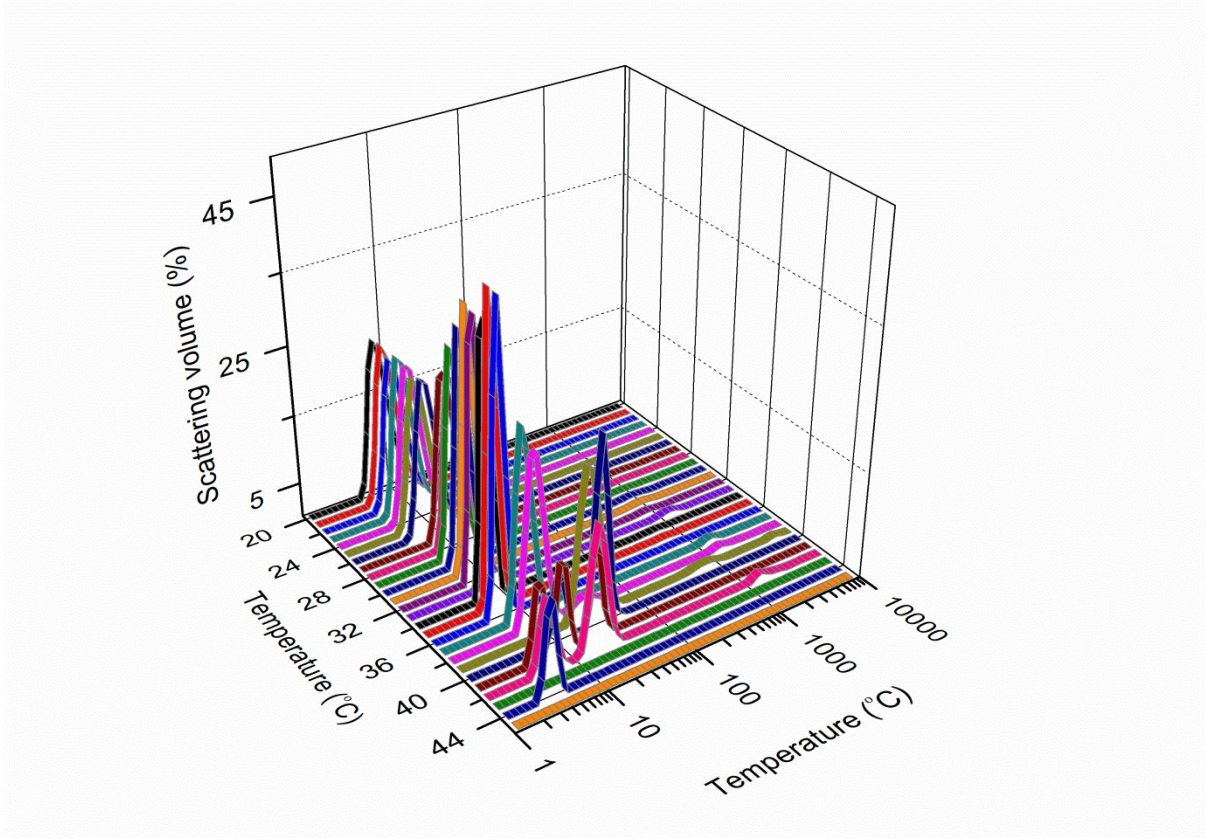

Figure S10: Temperature scanned dynamic light scattering volume plot of P3. The polymer exists as a free chain until ca. 39 ^{o}C, when the polymer self-assembles into a micellar sized structure, but a slight increase in temperature to 41 ^{o}C caused the polymer chains to self-aggregate.

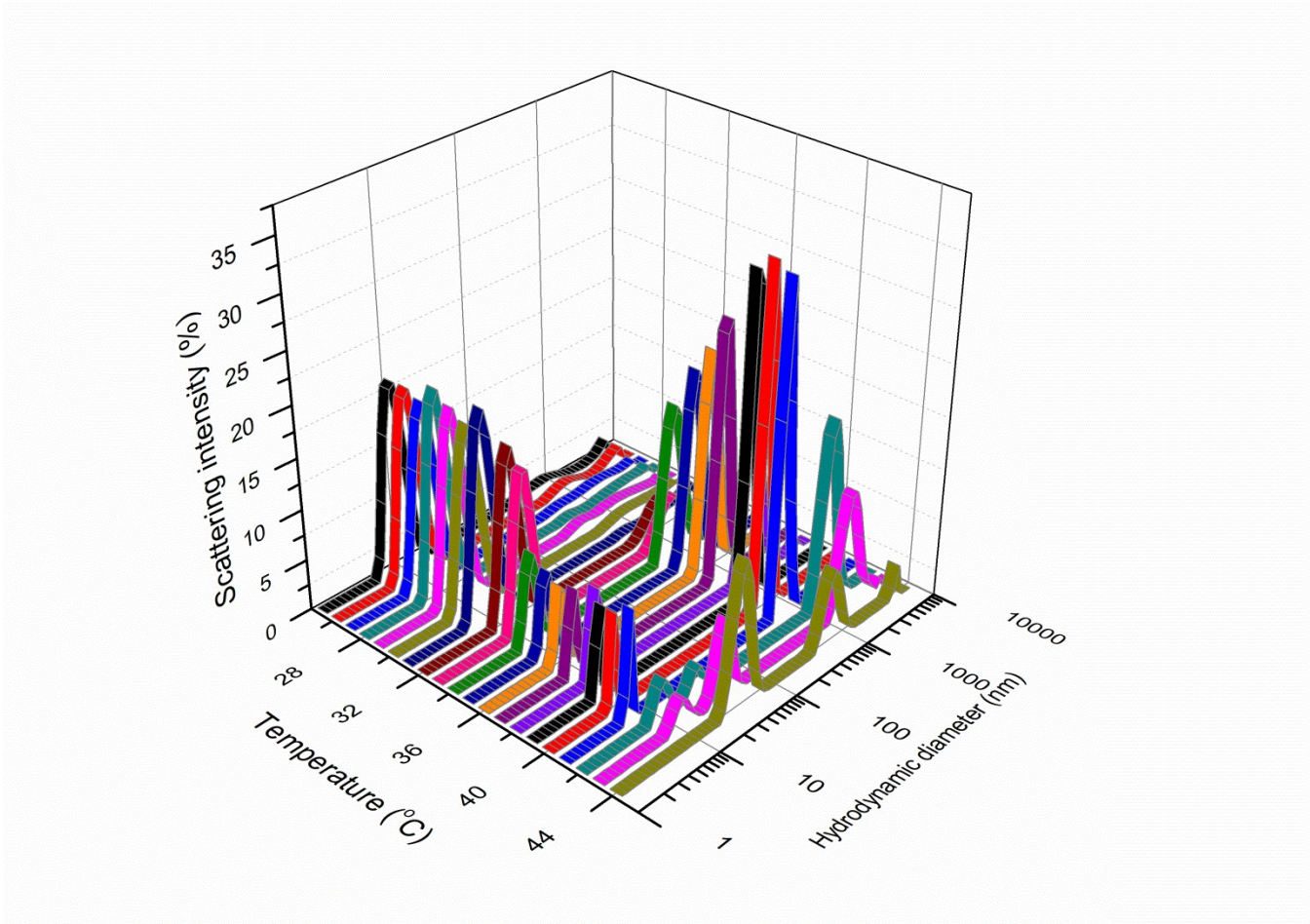

Figure S11: Intensity plot of P3 (*cf.* Fig. S10) which reveals the coexistence of free polymer and low concentrations of aggregates ca. 37 °C.

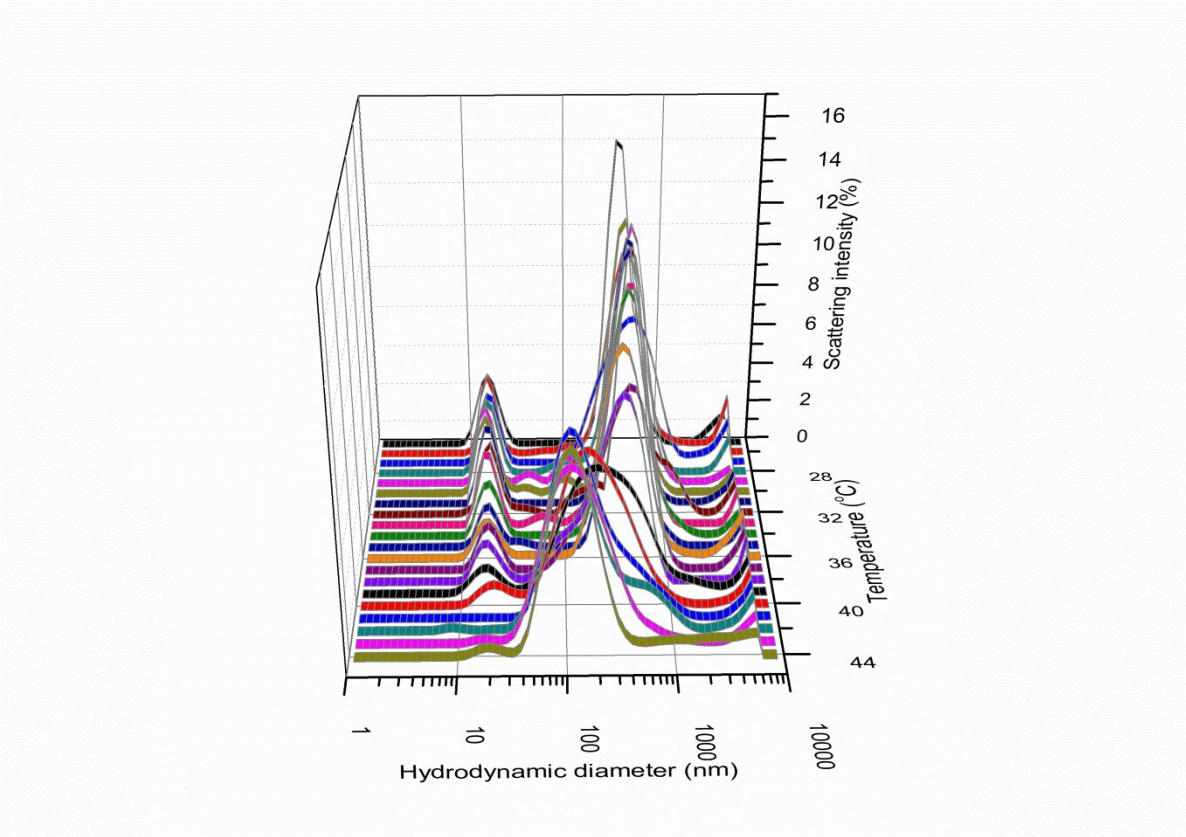

Figure S12: Intensity plot of P4 (*cf.* Fig. 3 in the main text) projected down the x-axis. This reveals that below the gelation point, the polymer exists as a high concentration of free chains (*cf.* Fig 3) and a low concentration of ca. 400 nm particles which can be attributed to flower like micelles. Above the gelation temperature the particles begin shrinking in size to ca. 100-200 nm and increasing in concentration as the free polymer also is incorporated into these structures.

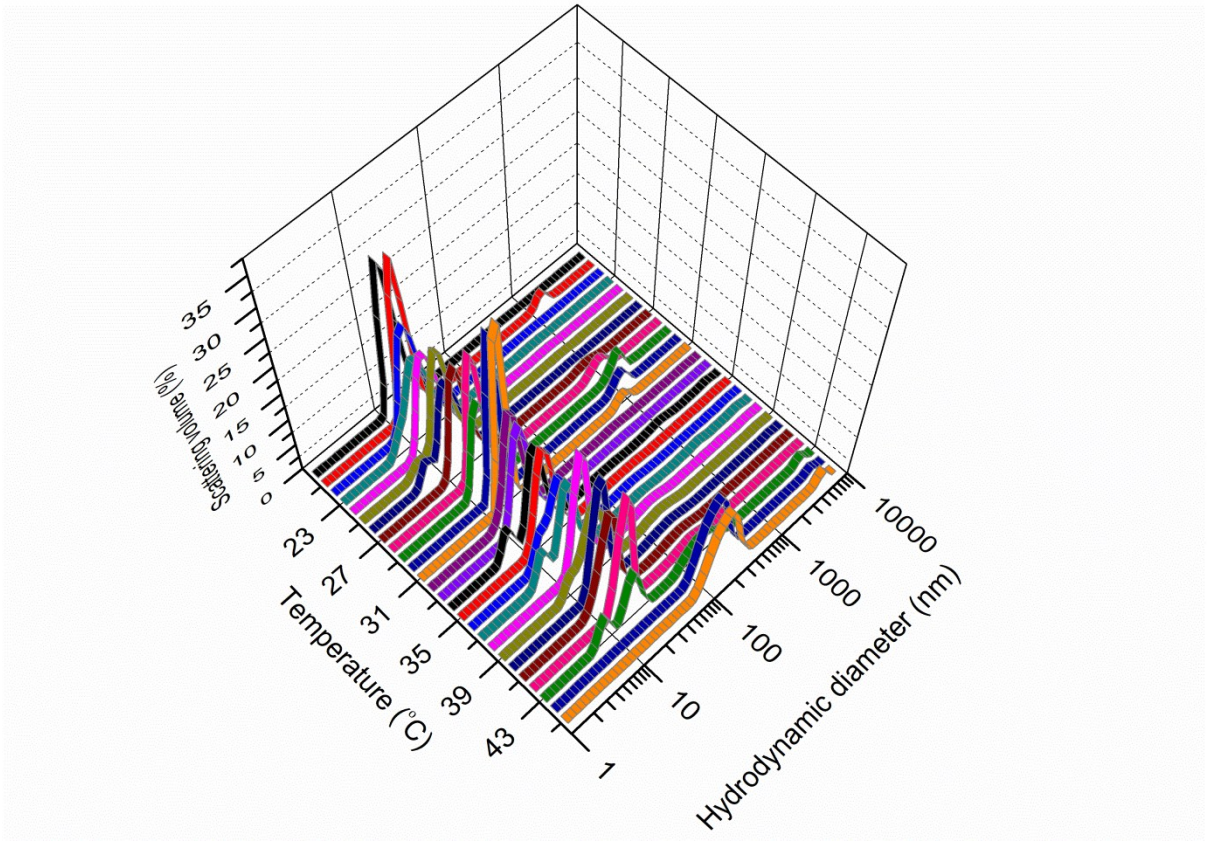

Figure S13: Temperature scanned dynamic light scattering volume plot of P5. The polymer exists as a free chain until ca. 43 ^{o}C, when the polymer self-assembles into a micellar sized structure.

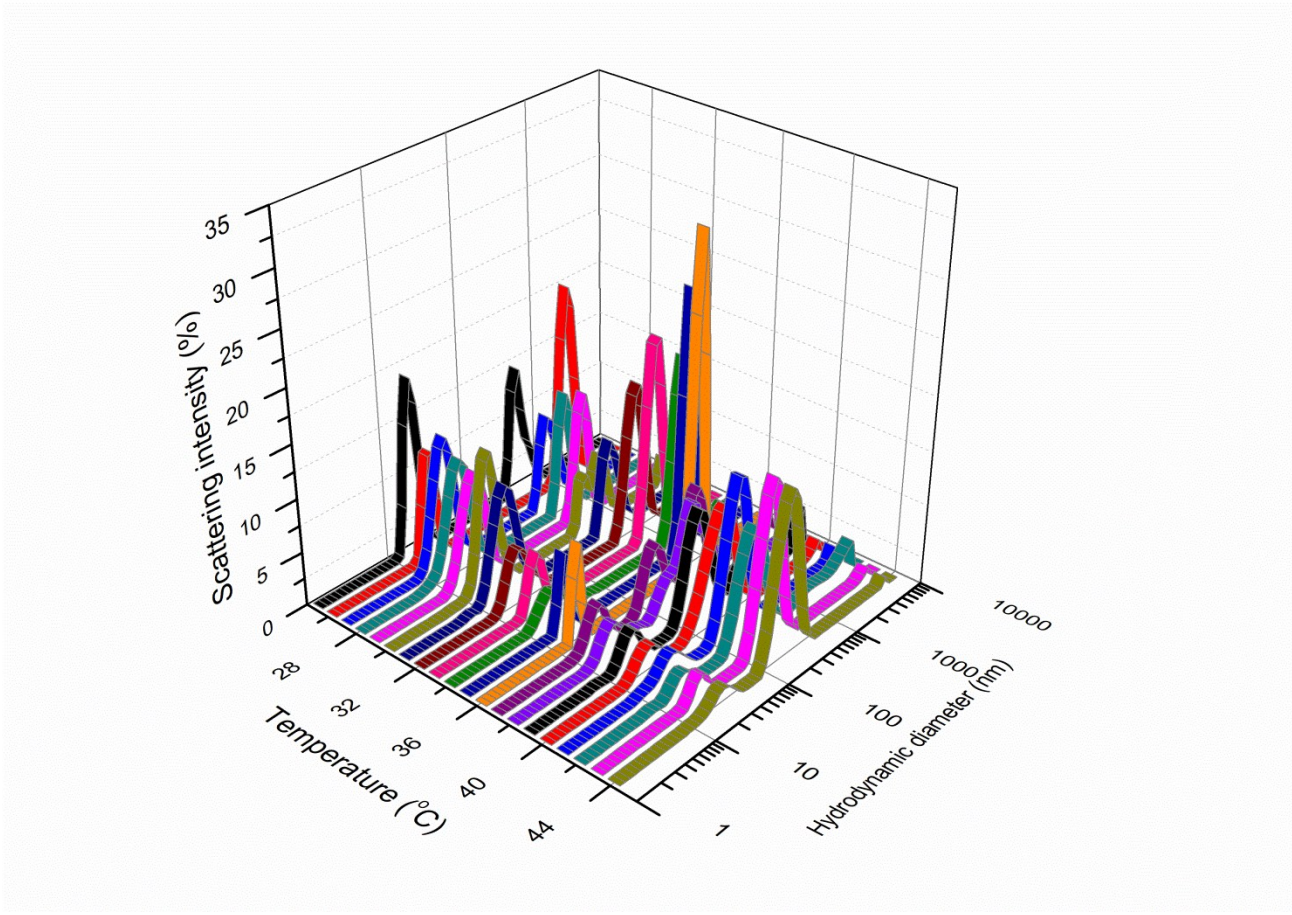

Figure S14: Intensity plot of P5 (*cf.* Fig. S13) which reveals similar behaviour to P4, but with a gelation point above human body temperature.

Relationship of Polymer Composition and Cloud Point

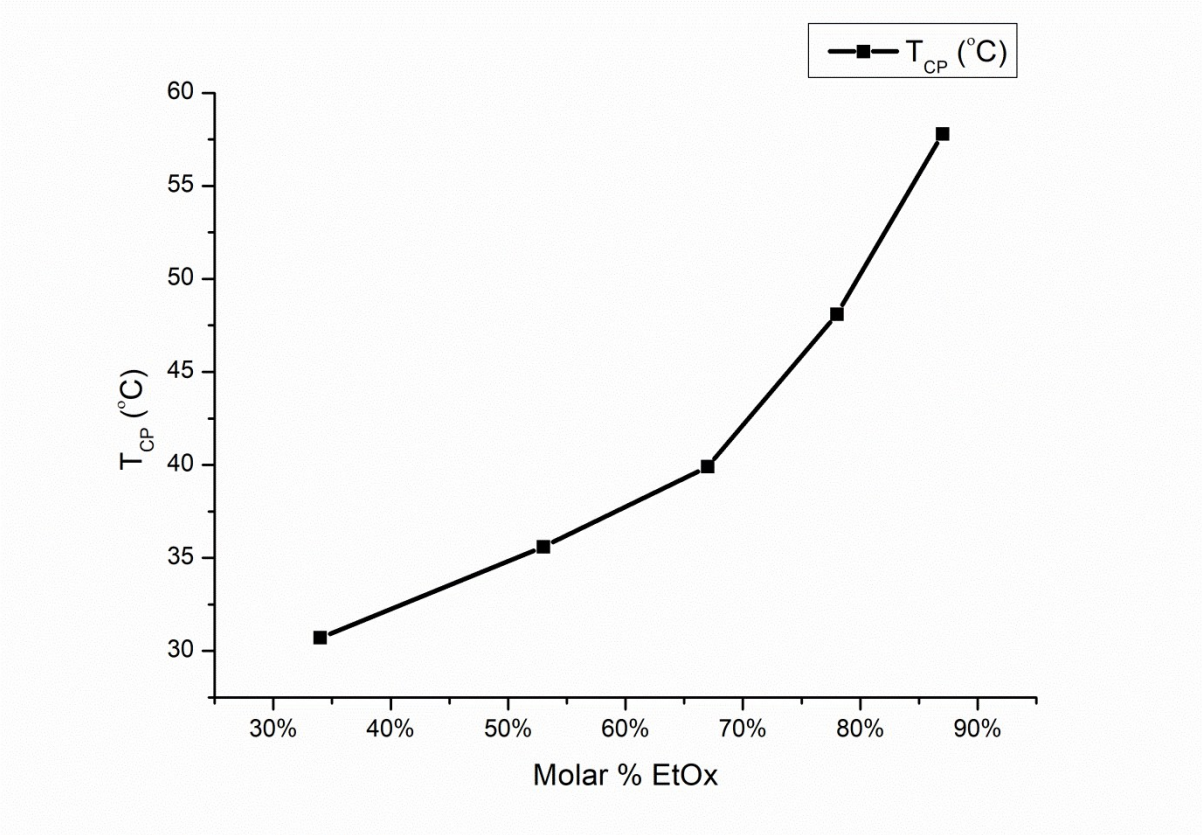

Figure S15: Transition temperatures as determined by DLS and turbimetry. For P1-3 the transitions are identical, but for P4 and P5 a window opens between transitions.

Additional Rheometry

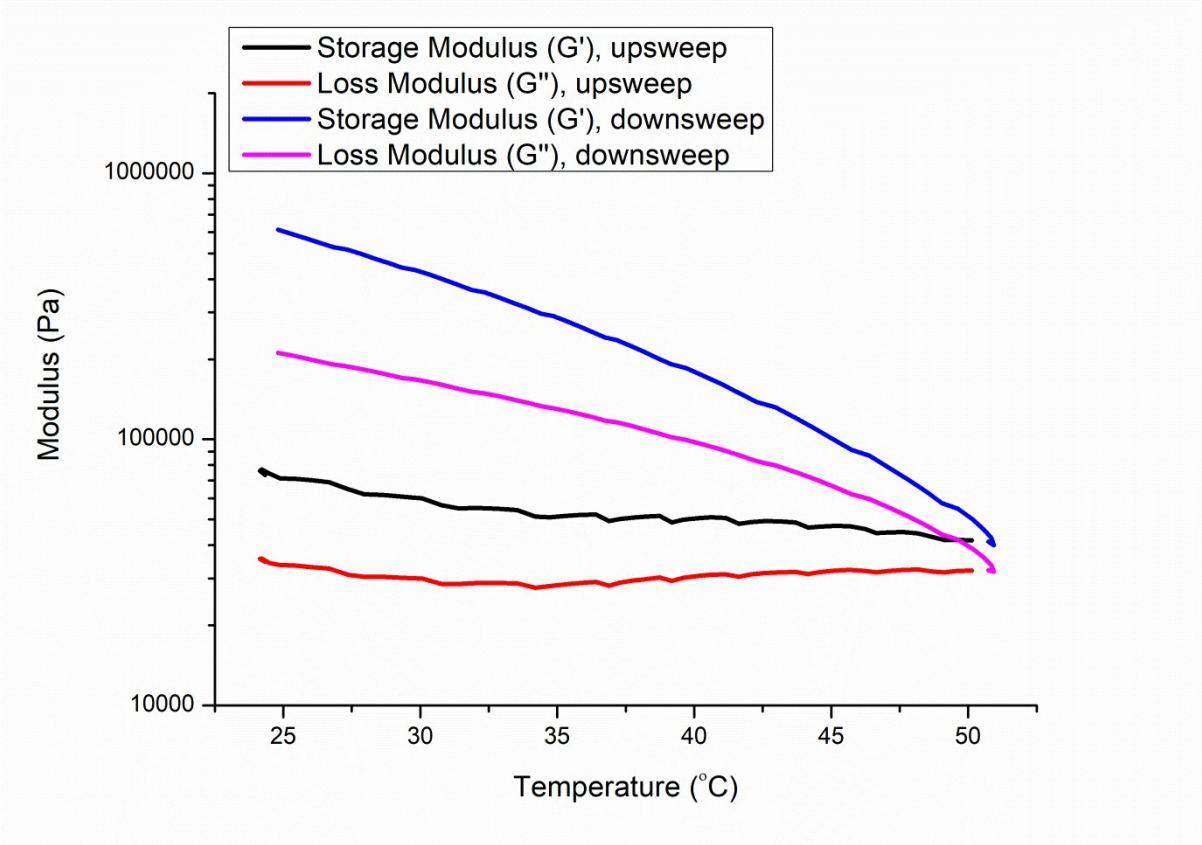

Figure S16: Second temperature sweep of a 20% aqueous P4 solution. Mechanical strength is only increased during the cooling cycle. It remains effectively constant during the heating cycle.

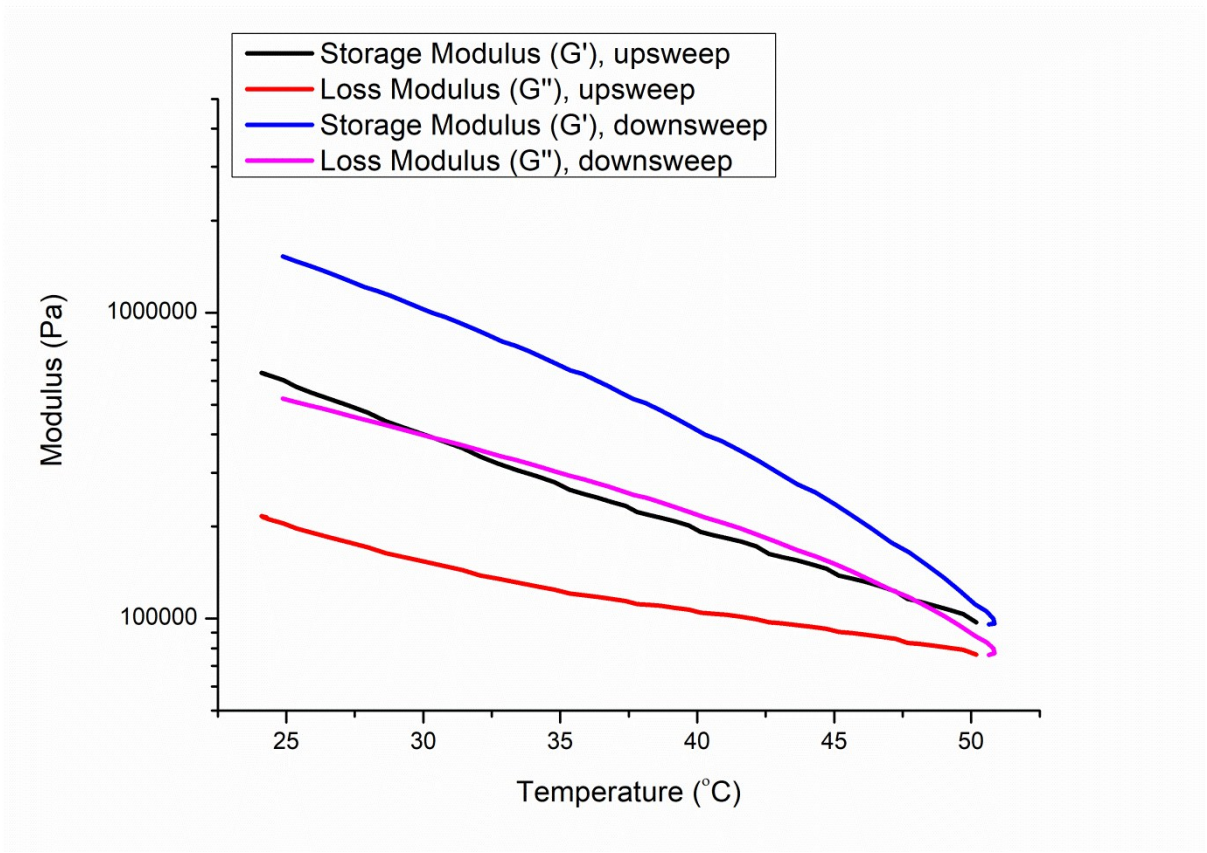

Figure S17: Third temperature sweep of a 20% aqueous P4 solution. Mechanical strength decreases during the heating cycle and increases during the cooling cycle. Further experiments were not possible as the vapour trap was exhausted after this experiment.

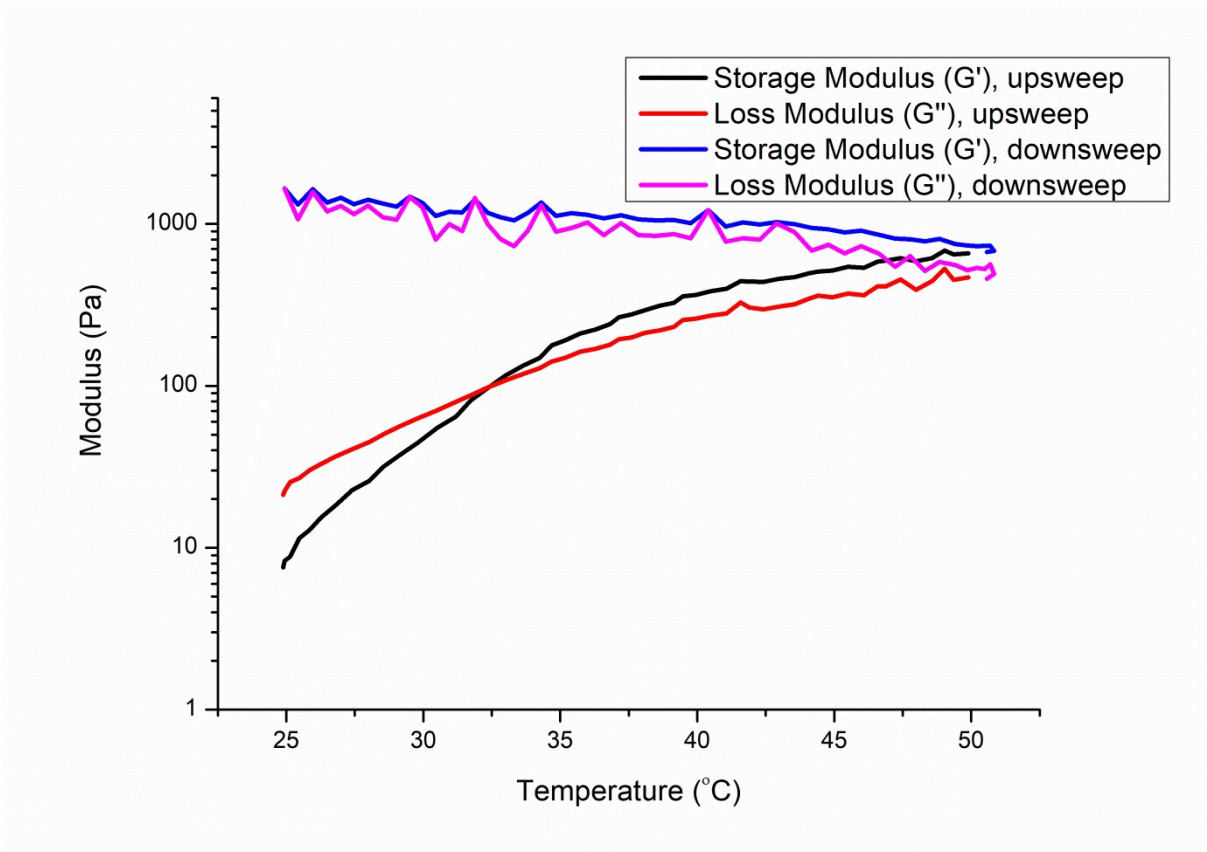

Figure S18: First temperature sweep of a 20% aqueous P5 solution. Similar behaviour to P4 is observed, but the hydrogel is weaker.

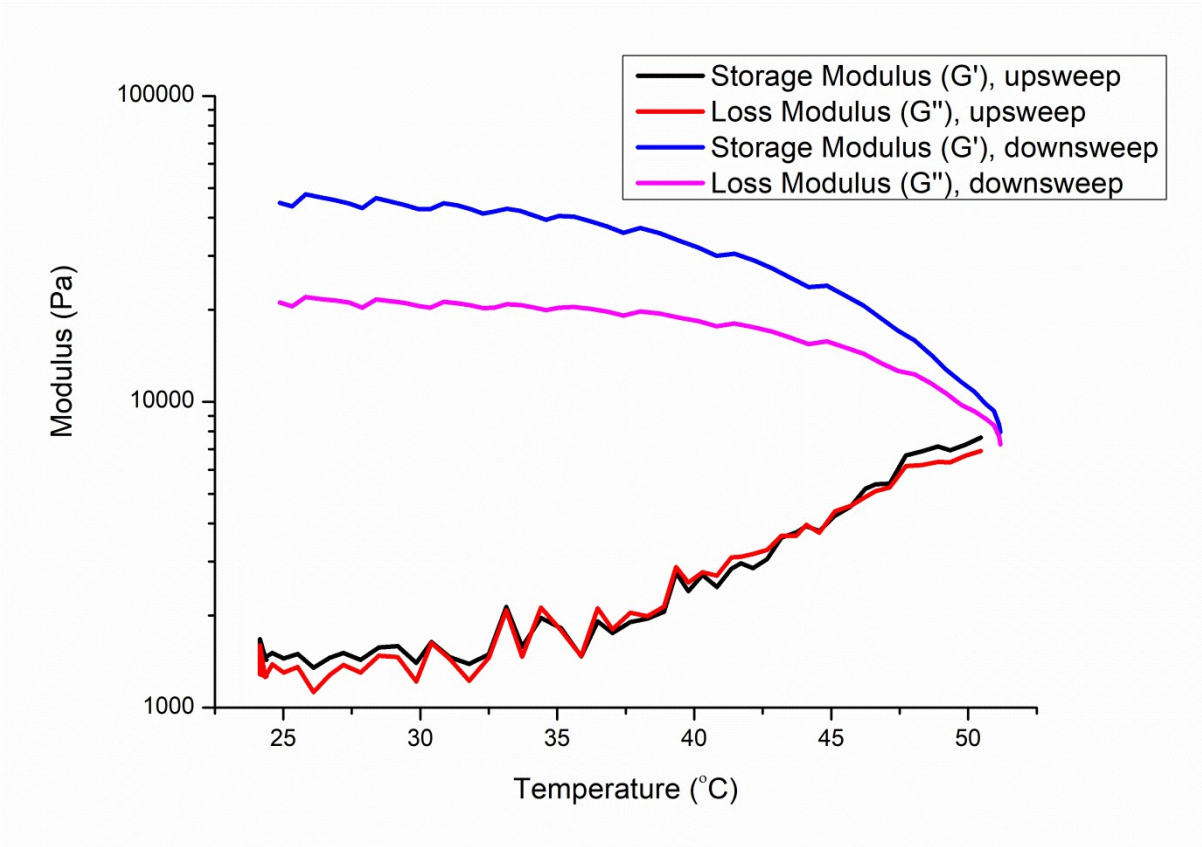

Figure S19: Second temperature sweep of a 20% aqueous P5 solution. Whilst weaker, unlike P4 (fig. S6) the hydrogel increases in strength during both cycles.

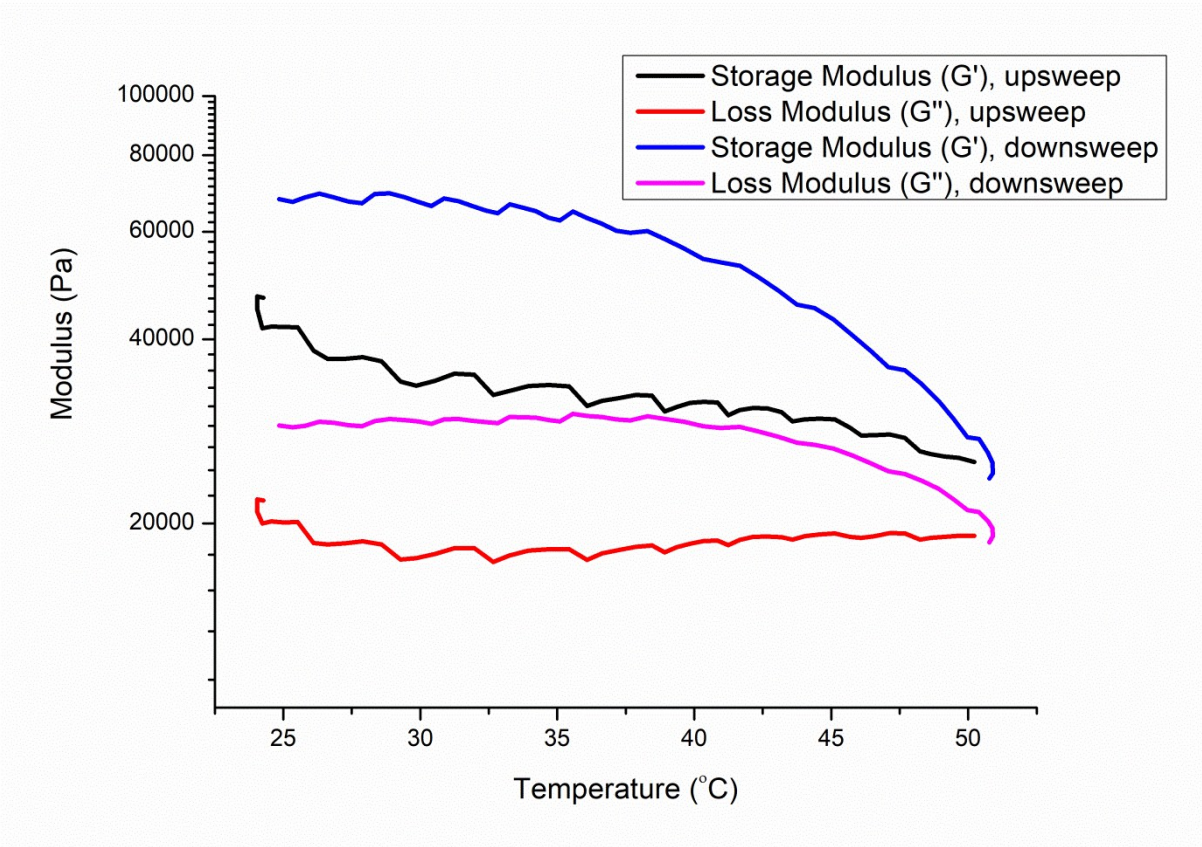

Figure S20: Third temperature sweep of a 20% aqueous P5 solution. Similar behaviour to P4's second heating cycle is observed, with the gel weakening at high temperatures.